HHS Public Access

Author manuscript

Cell Rep. Author manuscript; available in PMC 2016 March 07.

Published in final edited form as:

Cell Rep. 2013 July 25; 4(2): 316–326. doi:10.1016/j.celrep.2013.06.027.

Femtosecond Laser Ablation Reveals Antagonistic Sensory and Neuroendocrine Signaling that Underlie *C. elegans* Behavior and Development

Samuel H. Chung[1,2,3], **Anja Schmalz**[1], **Roanna C.H. Ruiz**[1,4], **Christopher V. Gabel**[#2,3,*], and **Eric Mazur**[#1,5]

[1]School of Engineering and Applied Sciences, Harvard University, 9 Oxford Street, Cambridge, MA 02138, USA

[2]Department of Physiology and Biophysics, Boston University School of Medicine, 72 E. Concord Street, Boston, MA 02118, USA

[3]Boston University Photonics Center, 8 Saint Mary's Street, Boston, MA 02215, USA

[4]Department of Biomedical Engineering, Cornell University, 101 Weill Hall, Ithaca, NY 14853, USA

[5]Department of Physics, Harvard University, 9 Oxford Street, Cambridge, MA 02138, USA

[#] These authors contributed equally to this work.

SUMMARY

The specific roles of neuronal subcellular components in behavior and development remain largely unknown, even though advances in molecular biology and conventional whole-cell laser ablation have greatly accelerated the identification of contributors at the molecular and cellular levels. We systematically applied femtosecond laser ablation, which has submicrometer resolution in vivo, to dissect the cell bodies, dendrites, or axons of a sensory neuron (ASJ) in *Caenorhabditis elegans* to determine their roles in modulating locomotion and the developmental decisions for dauer, a facultative, stress-resistant life stage. Our results indicate that the cell body sends out axonally mediated and hormonal signals in order to mediate these functions. Furthermore, our results suggest that antagonistic sensory dendritic signals primarily drive and switch polarity between the decisions to enter and exit dauer. Thus, the improved resolution of femtosecond laser ablation reveals a rich complexity of neuronal signaling at the subcellular level, including multiple neurite and hormonally mediated pathways dependent on life stage.

[*]Correspondence: cvgabel@bu.edu.

SUPPLEMENTAL INFORMATION

Supplemental Information includes Extended Results, Extended Discussion, Extended Experimental Procedures, three figures, and one table and can be found with this article online at http://dx.doi.org/10.1016/j.celrep.2013.06.027.

INTRODUCTION

Elucidation of the neuronal correlates of behavior and development has primarily proceeded by whole-cell laser ablation and localizing the expression of genes and activity of molecules with defined function (Bargmann, 1993; Bargmann and Avery, 1995). Although the nematode *Caenorhabditis elegans* represents an excellent model system for such study due to its invariant nervous system, amenable genetics, and powerful molecular biology (Brenner, 1974), most of the tools used to perturb neuronal function lack selective subcellular resolution. For instance, conventional laser ablation is limited to ablating whole cells, and the assignment of gene functions to a particular cell is complicated by multicell expression, although efforts are underway to mitigate this barrier (e.g., Senti et al., 2009). By contrast, femtosecond laser ablation, which has submicrometer precision in vivo, is capable of selective subcellular dissection for determining the correlates of behavior at a subcellular resolution (see Extended Experimental Procedures,). A strong body of evidence demonstrates cellular viability and minimal collateral damage following femtosecond laser ablation, with numerous examples of dissected subcellular components displaying normal calcium activity, mediating normal behavior, and readily regenerating (e.g., Pinan-Lucarre et al., 2012; Zhang et al., 2008). Here, we demonstrate the utility of this technique by systematic surgery on the subcellular components of the ASH and ASJ neurons, which have a similar, simple morphology and underlie several robust behaviors and developmental decisions mediated by a limited set of neurons. The ASH and ASJ belong to the amphids, a set of 12 bilateral sensory neurons each composed of a cell body, a dendrite terminating in sensory cilia, and an axon mediating the synaptic connections in the nerve ring (Figures 1A and 1B). Although the ASH forms connections to several neurons including the locomotory circuit, the ASJ neuron is postsynaptic to only four neurons (total of 5 synapses) and presynaptic to only the amphid neuron ASK (8 synapses) and interneuron PVQ (27 synapses) (White et al., 1986). The ASJ is also implicated in neuroendocrine signaling along multiple pathways (Carroll et al., 2006; Li and Kim, 2008). We systematically dissect (Figures 1C–1E and S1) the cell bodies, dendrites, or axons of the ASH and ASJ by femtosecond laser ablation to eliminate their signaling contribution, producing behavioral or developmental deficits that we identify by assay.

The nociceptive polymodal neuron ASH plays a role in mediating a variety of behaviors, including osmotic avoidance (Culotti and Russell, 1978). The roles of the ASH subcellular components in mediating osmotic avoidance are very well defined by genetic and molecular studies (de Bono and Maricq, 2005). Our postsurgery assays confirm these expected roles and establish the efficacy of the femtosecond laser ablation technique for systematically dissecting subcellular structures and determining their behavioral correlates.

The stomatin-like protein UNC-1 plays an important role in the pathways controlling sensitivity to multiple volatile anesthetics (e.g., halothane, isoflurane) (Rajaram et al., 1998; Sedensky et al., 2001), whose sites and mechanisms of action are poorly understood despite broad use in medicine for many decades (Campagna et al., 2003). Mutations disrupting *unc-1* lead to clear uncoordinated locomotion phenotypes in *C. elegans* (Brenner, 1974). Carroll et al. screened for suppressors of these broadly expressed genes, identified the ASJ-specific gene *ssu-1*, and suggested that the ASJ neuron secretes an SSU-1-modified signal to

affect UNC-1 function remotely (Carroll et al., 2006). Consistent with its suggested role in the ASJ, SSU-1 was identified as a cytosolic sulfotransferase (Hattori et al., 2006), a group of enzymes that catalyze the transfer of sulfate groups to remove toxins and metabolize molecules such as hormones (Strott, 2002). Using femtosecond laser ablation, we seek to test directly the hypothesis that the ASJ neuron secretes a signal along an SSU-1 pathway and to explore whether sensory or synaptic inputs modulate this pathway.

Under adverse conditions, *C. elegans* can develop into dauer, a facultative, developmentally arrested life stage specialized for survival. Dauer animals are profoundly different from normally developing animals at the molecular, cellular, and organismal levels. *C. elegans* integrates information from environmental cues, including food and a dauer-inducing pheromone, along multiple pathways involving several neurons to regulate entry to and exit from dauer (Hu, 2007). The ASJ neuron plays a prominent role in the dauer decisions, promoting pheromone-induced dauer entry and dauer exit (Bargmann and Horvitz, 1991; Schackwitz et al., 1996), but the specific ASJ signaling that modulates the dauer decisions is currently ill-defined. One ASJ signaling pathway is mediated by DAF-11, a transmembrane guanylate cyclase in the dendritic cilia (Birnby et al., 2000; Schackwitz et al., 1996; Thomas et al., 1993). Previous studies have also implicated hormonal signaling, suggesting that the ASJ secretes signals promoting dauer exit (Hu, 2007). We performed surgery on the ASJ neuron in wild-type and *daf-11(sa195)* animals to explore what dendritic and axonal signaling regulate the ASJ-mediated dauer pathways and to test the hypothesis that the ASJ neuron secretes a hormonal dauer exit signal.

Our results reveal a rich complexity of signaling within a single neuron and define distinct subcellular pathways for ASJ-mediated behaviors and development. Although multiple neurons and pathways are involved in the behaviors and development under study, and multiple models can be generated from our data, we endeavored to find the simplest model for ASJ signaling that can account for our data. In the text below, surgeries occur on the ASJ neuron unless otherwise noted. The roles of some subcellular components and the modality of some signals can be inferred from specific results. We present these interpretations alongside the experimental results. The roles of the cell body and the dendrite (summarized in Table 1) in the dauer decisions are identified by comparing results from multiple surgeries and assays. We save their exposition for the Discussion section.

RESULTS

Femtosecond Laser Ablation Confirms that the ASH Cell Body, Dendrite, and Axon Mediate the Osmotic Avoidance Behavior

Although the femtosecond laser ablation technique in *C. elegans* is well established (see Extended Experimental Procedures), the systematic application of femtosecond ablation to dissect subcellular structures for determining their behavioral correlates, the subject of our study, is relatively untried. Thus, we first sought to confirm the efficacy of the technique by application to a well-understood neuron and associated behavior—the ASH and osmotic avoidance. A plethora of genetic and molecular studies (reviewed in de Bono and Maricq, 2005) strongly supports a model where the osmotic avoidance behavior is mediated by ASH ciliary sensation and transmission of the nociceptive signal through the dendrite and axon to

the postsynaptic partners. This signal is then passed down to motor neurons that trigger an escape response to avoid regions of high osmolarity. We therefore expect that surgery on the left and right (L+R) ASH cell body, dendrite, or axon would abolish the osmotic avoidance behavior. As detailed in the Extended Results, our experiments confirm this existing model and establish the efficacy of the technique for determining the behavioral correlates of neuronal subcellular components.

ASJ Whole-Cell Ablation Rescues the *unc-1* Phenotype

The locomotion of L+R whole-cell-ablated *unc-1(e580)* animals significantly improved compared to mock animals (Figure 2A). Postsurgery animals exhibit both cleanly sinusoidal and kinked locomotion, indicating an incomplete restoration of coordinated locomotion. To quantify locomotion rescue, we measured the crawling speed of N2 wild-type, genetically rescued *ssu-1; unc-1*, mock-ablated *unc-1*, and whole-cell-ablated *unc-1* animals following surgery in L1 (Figure 2B). Among strains tested, N2 animals crawl the fastest, and *unc-1* mock-ablated animals crawl the slowest, with hardly any forward movement. Genetically rescued and whole-cell-ablated *unc-1* animals crawl significantly ($p < 10^{-4}$) faster than *unc-1* mock-ablated animals, but about 60% slower than N2 animals. Postsurgery *unc-1* animals display a major recovery of locomotion between the 20 and 44 hr assays, during which their speed increases from 5% to 30% of N2 crawling speed. We next investigated the effect of single- and double-sided whole-cell ablation. Unlike L+R whole-cell ablations, neither L nor R whole-cell ablation produces a significant difference in crawling speed from mock surgery (Figure 2C). We also investigated whether mutation of *ssu-1* and ASJ ablation rescue locomotion by coincident mechanism. The crawling speed of L+R, L, and R whole-cell-ablated *ssu-1; unc-1* animals is not statistically different from mock-ablated *ssu-1; unc-1* animals nor from L+R whole-cell-ablated *unc-1* animals (Figure 2C). Together with ASJ-specific expression of *ssu-1* (Carroll et al., 2006), this suggests that the rescue by whole-cell ablation is likely effected by nonspecific elimination of SSU-1. Thus, our results from whole-cell ablations indicate that the ASJ neurons are necessary for and redundantly mediate the *unc-1* phenotype via an SSU-1 pathway.

Next, we examined the contributions of the dendrites and axons to the *unc-1* signaling pathway. To reduce axonal regeneration that occurs vigorously in the larval stages (Gabel et al., 2008), we performed surgery in the late L4 stage, which is also the latest time that UNC-1 is required for coordinated locomotion (Hecht et al., 1996). Subsequent locomotion assays yield two findings. First, animals that underwent whole-cell ablations in L4 crawl significantly ($p < 10^{-4}$) faster than mock-ablated animals (Figure 2D), although L4 surgery produces a smaller recovery than L1 surgery (Figure 2C). These data indicate that SSU-1 is required through development to maintain the *unc-1* phenotype. Second, unlike whole-cell-ablated animals, dendrite-cut and axon-cut animals do not crawl significantly faster than mock-ablated animals. In fact, their crawling speed is slightly but significantly slower ($p < 10^{-4}$), possibly due to an increase in the time spent crawling backward. We confirmed these observations by performing surgery earlier in development in *dlk-1; unc-1* double mutants that exhibit reduced axon regeneration (Hammarlund et al., 2009). Dendrite-cut and axon-cut animals exhibit no locomotion recovery during the 3 days following surgery (Figure S2A). The same ASJ surgeries on wild-type animals have no significant effect on crawling

speed, eliminating the possibility of collateral damage near the nerve ring (Figure S2B). The lack of an increase in crawling speed following axon surgery eliminates ASJ synaptic signaling as necessary for the *unc-1* phenotype and suggests that the signal mediating the *unc-1* phenotype is secreted from the ASJ cell body (yellow curved line in Figure 5A). If the signal were transmitted synaptically, we would expect a rescue of locomotion following axon surgery. SSU-1 is localized to the ASJ neurons, suggesting that the outgoing signal is modified by SSU-1 prior to secretion, either directly or indirectly (Carroll et al., 2006). In summary, our results from axon surgeries support the hypothesis that the ASJ cell body mediates the *unc-1* phenotype via hormonal signaling.

ASJ Whole-Cell, Dendrite, or Axon Surgeries Reduce Dauer Entry in *daf-11*

Guanylate cyclases are a family of conserved enzymes that catalyze the conversion of guanosine triphosphate to cyclic guanosine monophosphate (cGMP), a secondary messenger regulating numerous processes from blood pressure to phototransduction in mammals (Potter, 2011). In *C. elegans*, the transmembrane guanylate cyclase DAF-11 is present in the dendritic cilia of the ASJ and four other amphid neurons where it mediates chemotaxis, avoidance to multiple olfactory and gustatory cues, and one of the dauer entry pathways (Birnby et al., 2000; Vowels and Thomas, 1994). At 25°C, most *daf-11(sa195)* mutants enter dauer even under fertile conditions, whereas at 15°C, most develop normally (Thomas et al., 1993). Schackwitz et al. demonstrated by conventional laser ablation that the ASJ neuron mediates *daf-11* constitutive and wild-type pheromone-induced dauer entry at 25°C (Schackwitz et al., 1996).

We performed surgeries at 4 hr after hatching on the ASJ cell body, dendrite, and axon to determine their roles in *daf-11* dauer entry signaling. When assayed at 25°C, significantly ($p < 10^{-4}$) lower percentages of L+R whole-cell-ablated and L+R dendrite-cut *daf-11* mutants enter dauer compared to mock animals (Figure 3A). Our results indicate signals in the dendrite (Table 1, row 4) and from the cell body that promote dauer entry. Although conventional whole-cell ablation at 2 hr after hatching yields a decrease of 60% in the dauer entry rate (Schackwitz et al., 1996), after our whole-cell ablations, dauer entry decreases by only 35%. The reduced effect is likely due to the later time of our surgeries; in some experiments (see below), the later time of surgery appears to eliminate the surgical effect entirely. L+R axon cuts in *daf-11* mutants do not reduce dauer entry (32 out of 33 animals enter dauer), but strong axon regeneration to the nerve ring occurs within hours of ablation, potentially restoring neuronal signaling. To reduce axon regeneration and possible functional recovery (Hammarlund et al., 2009), we used a *dlk-1; daf-11* double mutant, and we assayed at 24.5°C to reduce this strain's unusually strong dauer entry behavior. L+R axon cuts significantly ($p < 10^{-4}$) lower the *dlk-1; daf-11* dauer entry percentage to a similar degree as L+R whole-cell or dendrite surgeries (Figure 3A), suggesting an axonally mediated signal from the ASJ cell body that promotes dauer entry. Although amphid axon guidance defects also suppress *daf-11* dauer entry (Zallen et al., 1999) and suggest an axonally mediated dauer entry signal from the ASJ, our results provide direct evidence for this modality. Interestingly, surgeries on the ASK or PVQ neurons, the postsynaptic partners of the ASJ, did not significantly change dauer entry, suggesting that the signal might be secreted from the ASJ axon rather than synaptically mediated (see Extended Results). In

summary, our results indicate signals promoting *daf-11* dauer entry in the ASJ cell body, dendrite, and axon.

We also investigated the effect of single-sided ASJ surgeries on dauer entry at 25°C. Single-sided surgeries on the ASJ cell body, dendrite, or axon do not produce significant changes from their respective mock-ablated dauer entry percentages at 25°C (Figure 3A), in contrast to results from a previous study involving whole-cell ablation earlier in development (Schackwitz et al., 1996). Thus, our data indicate that by 4 hr after hatching, the ASJ cell bodies redundantly promote *daf-11* dauer entry at 25°C.

At 15°C, most *daf-11* mutants develop normally (Vowels and Thomas, 1994), and all our surgeries produce no significant changes in behavior from mock ablations (Figure 3A). This suggests that the signaling in the ASJ cell body, dendrite, and axon that promotes dauer entry at 25°C is reduced or blocked at 15°C. The data also do not indicate any repression of dauer entry by the subcellular components of the ASJ neuron.

ASJ Surgeries Delay Wild-Type Dauer Exit but Trigger Dauer Exit in *daf-11*

The ASJ neuron promotes dauer exit in wild-type animals (Bargmann and Horvitz, 1991), and most *daf-11* mutations prevent dauer exit, implicating dendritic involvement (Thomas, 1993). In addition, several studies have posited that hormones might synchronize wild-type dauer exit organismally (Avery et al., 1993; Tissenbaum et al., 2000; Wang and Kim, 2003), suggesting that the ASJ neuron might secrete a dauer exit signal. To elucidate the ASJ signaling pathways controlling dauer exit, we performed surgery on the ASJ neuron in wild-type and *daf-11(sa195)* dauers and noted changes in dauer exit on seeded plates. We assayed animals immediately after surgery, scoring dauer exit by pharyngeal pumping (Cassada and Russell, 1975); the Extended Results also describes results from an assay performed 1.5 days after cell body surgery. Wild-type animals exit dauer rapidly at a mean exit time of 3 hr after introduction to the seeded plate, and all types of surgeries we performed on the ASJ neuron significantly ($p < 10^{-4}$) delay wild-type dauer exit compared to mock-ablated animals (Figure 3B, solid curves). L+R axon-cut wild-type animals exited dauer rapidly but about 2-3 hr after mock-ablated animals. The short delay and rapid exit following axon surgery suggest that the signal from the ASJ promoting dauer exit is secreted (upper yellow curved line in Figure 5C) because we would expect a larger impact on dauer exit if it were necessary for the signal to be axonally mediated. The statistically significant delay, however, also suggests that the axon carries a signal playing a relatively small role in promoting dauer exit. L+R whole-cell ablations, dendrite cuts, and dendrite plus axon cuts in wild-type animals produce considerably longer delays with slower and less-complete exit than in mock-ablated or axon-cut wild-type animals, suggesting that signals in the dendrite and from the cell body have a more prominent role in promoting dauer exit than the axonal signal. Thus, each surgery produces a distinct delay in wild-type dauer exit, suggesting distinct excitatory signals associated with the cell body, dendrite (Table 1, row 5), and axon.

Mutants in *daf-11* exhibit varying degrees of defects in dauer exit; *daf-11(sa195)* has one of the strongest defects, and virtually no animals recover, even at 15°C (Vowels and Thomas, 1994). In agreement, none of the mock-ablated *daf-11* mutants exited dauer in our experiments on seeded plates. L+R whole-cell-ablated *daf-11* mutants also do not exit dauer.

In contrast, the other surgeries we performed on the ASJ neuron trigger dauer exit and produce a significant ($p < 10^{-4}$) difference from mock behavior (Figure 3B, dashed curves). L+R axon cuts trigger a slower dauer exit than L+R dendrite cuts or L+R dendrite plus axon cuts. This suggests that inhibitory signals exist in the dendrite and axon, but the dendritic signals have a more prominent role in repressing dauer exit than the axonal signal. In addition, following L+R dendrite cuts, the dauer exit of wild-type and *daf-11* animals is statistically indistinguishable, indicating that the *daf-11* defect in dauer exit is localized to the ASJ dendritic cilia, as previously suggested by Birnby et al. (2000). Thus, surgeries on the ASJ dendrite and axon can lead to resumption of dauer exit in *daf-11* mutants at rates similar to postsurgery wild-type dauer exit, suggesting that the ASJ dendrite (Table 1, row 6) and axon transmit signals to repress dauer exit.

Next, we examined the role of food by assaying the dauer exit of animals held in nematode growth medium (NGM) buffer with and without OP50. Following established protocol by Bargmann and Horvitz (1991), we cultivated and assayed animals 1 day after surgery, scoring dauer exit by SDS sensitivity 7 hr after introduction to OP50 (see Experimental Procedures). We kept wild-type animals at 20°C and *daf-11* animals at 25°C. Our results from the liquid assays with OP50 (Figures 4A and 4B, shaded regions) confirm results from the seeded plates. For wild-type animals in buffer with OP50, L+R whole-cell ablation and L+R dendrite cuts reduce dauer exit, whereas L+R axon cuts do not produce a significant effect on dauer exit. These results highlight the prominent roles of the cell body and the dendrite (Table 1, row 5) in promoting wild-type dauer exit and suggest that the dauer exit signal is secreted. For *daf-11* mutants in buffer with OP50, only L+R dendrite cuts lead to dauer exit, confirming an inhibitory signal in the dendrite (Table 1, row 6). Liquid assays without OP50 (Figures 4A and 4B, unshaded regions) yield a surprising finding. Even without OP50, most *daf-11* mutants with L+R dendrite surgery have initiated dauer exit by 1 day after surgery, as evidenced by SDS sensitivity (Figure 4B), lightened tissue (Figure 4C), and nonquiescent behavior. After 3 days, many have radially thickened and some carry eggs (Figure 4D), indicating further development in the absence of food. Also, when placed on seeded plates, these pale or further-developed animals immediately commence pharyngeal pumping, in contrast to mock-ablated dauers, which initiate pumping after a 1 hr delay (Figure 3B; Cassada and Russell, 1975). Because the dauer exit behaviors on seeded plates of wild-type and *daf-11* animals following L+R dendrite surgery are so similar (Figure 3B), we performed the L+R dendrite surgery again on wild-type animals while holding them at 25°C. By 3 days after surgery, seven out of eight L+R dendrite-cut wild-type animals also exited dauer in NGM buffer without OP50, indicating that, given sufficient time, dendrite cuts can also trigger dauer exit in wild-type animals. Thus, in addition to confirming our results from seeded plates, we find that in the absence of OP50, the ASJ dendrite plays a role in repressing dauer exit in both wild-type and *daf-11* animals (Table 1, rows 7 and 8). Finally, ablation of the postsynaptic partners of the ASJ suggests that they do not play a prominent role in ASJ-mediated dauer exit (see Extended Results), consistent with results from axon surgeries indicating a limited role.

In most of our dauer exit assays, axon cuts yield a smaller change in behavior compared to whole-cell ablations (Figures 3B, 4A, and 4B). These results indicate that the primary

outgoing signals from the ASJ cell body for dauer exit are secreted rather than synaptically mediated. Axon cuts, however, do yield relatively small changes in dauer exit behavior indicating a role for the axon in transmitting signals that promote (wild-type) and repress (*daf-11*) dauer exit. These axonal signals appear to modulate dauer exit behavior alongside, but to a lesser degree than, dendrite signals (Figure 3B). Although our experiments do not establish whether the axonal signals are incoming or outgoing, for simplicity, we suggest a working model where axonal inputs are integrated with dendritic inputs in the ASJ cell body, which then secretes outgoing dauer exit signals (Figure 5C).

DISCUSSION

We have performed femtosecond laser ablation to dissect out the subcellular parts of two neurons in *C. elegans* to define their roles in behavior and development. Our results verify that the ASH cell body, dendrite, and axon transmit a signal mediating osmotic avoidance behavior. These results substantiate the efficacy of the femtosecond laser ablation technique for dissecting subcellular neuronal signaling, which was established in previous studies (see Extended Experimental Procedures). We also dissected the ASJ subcellular components to determine their roles in SSU-1 signaling of the *unc-1* locomotion phenotype. From the axon surgeries, we conclude that the ASJ cell body secretes an SSU-1-modified signal rather than transmitting it synaptically (Figure 5A). Finally, by integrating results from multiple surgeries and dauer assays, we can develop a more comprehensive model for dauer entry and exit decisions (Figures 5B and 5C). As we discuss below, we conclude that the ASJ cell body sends out an axonally mediated signal promoting dauer entry and secretes signals promoting and repressing dauer exit. We also conclude that the ASJ dendrite transmits antagonistic sensory signals that primarily drive and switch polarity between the dauer decisions.

Neuroendocrine Signaling Underlies the unc-1 Phenotype

Numerous experiments implicate UNC-1 as a molecular target for volatile anesthetics (e.g., Morgan et al., 1990; Rajaram et al., 1998). Elucidating the regulators of *unc-1* might provide insight into the role of *unc-1* in the pathways controlling anesthetic action. Although the identification of *ssu-1(fc73)* as a suppressor of the *unc-1* phenotype provided a genetic route to investigate the properties of *unc-1*, the specific means of suppression were not directly established (Carroll et al., 2006). Using femtosecond laser ablation of the ASJ neuron, we sought to ascertain the signaling modality underlying *ssu-1* suppression of the *unc-1* phenotype and to explore whether sensory or synaptic inputs modulate this pathway. Our results indicate that *ssu-1* mediation of the *unc-1* phenotype is reversible late in development and opens the door to studies of *unc-1* regulation dynamics, which could yield deeper insights into the mechanisms by which volatile anesthetics act on *unc-1*. Our results also indicate that the ASJ cell body redundantly mediates the *unc-1* phenotype by secretion of an SSU-1-modified signal (Figure 5A). Although this signal's molecular identity, relation to SSU-1 (direct or indirect modification), and mode of action remain unknown, possible candidate molecules include sterols, which are substrates for sulfotransferases, important players in dauer pathways, and highly conserved regulators of metabolism and homeostasis (Strott, 2002; Wollam and Antebi, 2011).

The Role of the ASJ Cell Body in Dauer Entry and Exit

Previous experiments using conventional whole-cell laser ablation have shown that the ASJ neuron promotes *daf-11* dauer entry at 25°C, wild-type pheromone-induced dauer entry, and wild-type dauer exit (Bargmann and Horvitz, 1991; Schackwitz et al., 1996). In agreement, our results strongly confirm that the ASJ cell body promotes dauer entry and dauer exit (Figures 5B and 5C) but suggest that the role of the ASJ cell body in dauer exit is more complex. First, wild-type dauer exit behavior following whole-cell ablation suggests that cells other than the ASJ promote a later and more gradual dauer exit (at 6–8 hr) than ASJ-mediated dauer exit (at 2–3 hr). Second, the dauer exit profiles of wild-type animals following dendrite cuts and following whole-cell ablations are not statistically different, with the divergence between 6 and 15 hr possibly due to the onset of rapid, ASJ-independent dauer exit (at 3 hr) mentioned earlier (Figure S3). We represent the signaling for this late, non-ASJ-mediated wild-type dauer exit by a “neutral” signal from cell body in Figure 5C. Third, compared to this late dauer exit (at 6–8 hr), which is also exhibited by *daf-11* dendrite-cut mutants, the lack of dauer exit in *daf-11* mock animals (Figure 3B) suggests that the ASJ cell body outputs a dauer maintenance signal (i.e., inhibitory signal from cell body in Figure 5C). Although our model captures the primary features of our data, certain experimental results are paradoxical and suggest additional signaling complexity beyond our model. First, ASJ whole-cell ablations, which should eliminate the inhibitory ASJ dauer exit signal, do not yield dauer exit in *daf-11* mutants (Figure 3B). This result is most readily resolved if other cells expressing *daf-11* (ASI, ASK, AWB, or AWC; Birnby et al., 2000) also repress dauer exit. Consistent with this interpretation, we demonstrate that the ASK represses dauer exit in wild-type animals in NGM buffer without OP50 (see Table S1). Second, whole-cell ablation and neurite surgeries produce different outcomes in *daf-11* dauer exit. One possible explanation is that eliminating the neurite inhibitory signal by surgery could trigger the cell body to promote dauer exit (signal 1 in Figure 5C) and stop the cell body from repressing dauer exit (signal 3 in Figure 5C). Both these effects may be required to trigger *daf-11* dauer exit. Full elucidation of the dauer exit signaling will likely require identifying and disrupting the specific ASJ signals and generating models of greater complexity, highlighting the need for integrating subcellular-resolution dissection and conventional molecular and genetic techniques. In summary, our results demonstrate that the ASJ cell body sends out signals promoting dauer entry and promoting dauer exit. Results from dauer exit assays on seeded plates also suggest that the ASJ cell body represses dauer exit and that other cells can supplement or compensate the ASJ neuron in promoting and repressing dauer exit.

Our study provides direct evidence identifying the modality of the outgoing ASJ signals for dauer decisions. Although our findings establish that the signal for dauer entry is axonally mediated, whereas the signal(s) for dauer exit is secreted, many details of the downstream signaling require clarification to produce a complete model. Excitatory and inhibitory signals from multiple neurons (e.g., ADF, ASI, ASG, ASJ, and ASK) modulate dauer entry and are integrated to produce a coherent organismal response (Bargmann and Horvitz, 1991). Determining which cell(s) processes these signals (e.g., XXX) will be crucial in fully illuminating the dauer entry signaling pathways (Ohkura et al., 2003). In contrast to dauer entry, which is modulated by multiple sensory neurons, the ASJ appears to play the primary

role in triggering rapid dauer exit. A secreted signal, which can synchronize organism-wide dauer exit, is consistent with expected players in dauer exit, which include several neuropeptides (see Extended Discussion), TGF-β, and sterols (Hu, 2007). Two outstanding questions here are the molecular identity of the signal, and whether the signal is further processed or altered by other cells or if it directly causes the somatic cells to resume development.

The ASJ Dendrite Transmits Multiple Signals to Drive the Dauer Decisions

The ASJ neuron promotes both dauer entry and exit (our results; Bargmann and Horvitz, 1991; Schackwitz et al., 1996), but the ASJ dendritic sensory signaling that modulates dauer entry and exit is currently ill-defined. Previous experiments seeking to illuminate the specific ASJ dendritic signaling, however, have yielded paradoxical results, which we summarize in Table 1. Under noninducing conditions (high-food and low-pheromone levels), *daf-11* mutants enter dauer, whereas wild-type animals do not (Vowels and Thomas, 1992), suggesting that DAF-11 might normally mediate a dendritic signal repressing dauer entry (Table 1, row 1). In contrast, cilium structure mutations render *daf-11* mutants dauer defective (Vowels and Thomas, 1992) and suggest an excitatory dendritic signal (Table 1, row 2). Conventional laser ablation of the sheath cell that surrounds the amphid cilia reduces dauer entry under pheromone (Vowels and Thomas, 1994), suggesting an excitatory dendritic signal (Table 1, row 3). We sought to clarify directly the ASJ dendritic signaling for dauer decisions by cutting L+R dendrites in both *daf-11* and wild-type animals and assaying both dauer entry (with OP50) and exit (with and without OP50) under otherwise similar environmental conditions. Our results show an excitatory signal for *daf-11* dauer entry (Table 1, row 4), an excitatory signal for wild-type dauer exit (row 5), an inhibitory signal for *daf-11* dauer exit (row 6), and if animals are held in buffer without OP50 for days, inhibitory signals for wild-type and *daf-11* dauer exit (rows 7 and 8). These experiments paradoxically suggest signals of opposite polarity; however, the continued presence of a dendritic signal after silencing a DAF-11-mediated signal indicates that there is more than one ASJ dendritic signal. In summary, the evidence strongly suggests that the ASJ dendrite transmits multiple signals, one mediated by DAF-11, to drive the dauer decisions based on specific sensory input and life stage.

The ASJ Dendrite Transmits Antagonistic Signals that Switch Polarity between Dauer Entry and Exit

Two observations guided us toward a model with two dendritic signals. First, *daf-11(sa195)*, which is the best null allele candidate (Birnby et al., 2000) and should eliminate the DAF-11-mediated signal, seems to switch the polarity of the dendritic signal (Table 1, rows 1→2 and 5→6), suggesting that there are (at least) two signals with opposite sign. Second, under otherwise similar conditions, the sign of the dendritic signal for dauer entry and dauer exit (Table 1, rows 1 and 5, and 4 and 6) is opposite, suggesting a switch in polarity during development. A model consistent with the data is shown in Figures 5B and 5C. Central to the model are antagonistic sensory signals in the ASJ dendrite that switch polarity between dauer entry and dauer exit. Wild-type animals integrate both sensory signals and can make appropriate dauer decisions under various environmental conditions. Mutants with *daf-11(sa195)* have a specific defect in their ASJ cilia that removes the sensory signals

repressing entry and promoting exit, and they are consequently dauer constitutive. The application of 8-bromo-cGMP (a membrane-permeant cGMP analog) suppresses *daf-11* and pheromone-mediated dauer entry but induces *daf-11* dauer exit (Birnby et al., 2000), suggesting that cGMP underlies the DAF-11-mediated dendritic signal repressing dauer entry and promoting dauer exit. Interestingly, in our model, the role of the DAF-11-mediated sensory signal in the dauer decisions (repressing entry, promoting exit) is consistent with the role of food, and the role of the non-DAF-11-mediated sensory signal in the dauer decisions (promoting entry, repressing exit) is consistent with the role of pheromone. We hypothesize that components of food and pheromone are the environmental cues transduced into the antagonistic dendritic sensory signals (left side of Figures 5B and 5C). Results from multiple experiments confirm key features of our model. One of the original studies involving dauer pheromone postulated the existence of multiple dendrite pathways after they observed that wild-type pheromone-induced dauer entry and the dauer entry of some dauer constitutive mutants, including *daf-11*, are both temperature sensitive. This led the authors to suggest that these mutants have a specific defect in their food signaling pathway that exposes, but does not impact, a separate pheromone signaling pathway (Golden and Riddle, 1984). Indeed, separate food and pheromone pathways, which are a prominent feature of our model, are consistent with published results showing that *daf-11* loss-of-function mutants are still pheromone sensitive (Golden and Riddle, 1984; Thomas et al., 1993). Also, a role in our model for DAF-11 in mediating a food (rather than a pheromone) pathway is confirmed by two of our observations. First, our model correctly predicts that in an environment without food, the dendritic signal for both wild-type and *daf-11* dauer exit should be inhibitory (Table 1, rows 7 and 8). Second, our model predicts that *daf-11* mutants are food insensitive for ASJ-mediated dauer behavior, which is consistent with results from our liquid dauer exit assays (note vertical symmetry of data in Figure 4B). In summary, our data and published observations support a model where the ASJ dendrite transmits antagonistic signals encoding sensory information to drive the dauer decisions.

Our observation that the ASJ dendritic signals primarily drive the dauer decisions suggests that the response of the ASJ cell body for dauer behavior is largely dictated by environmental cues sensed by the ASJ dendrite rather than sensory or metabolic information from other cells. The aggregate activity of various signaling molecules, such as insulin-like peptides, likely comprises a significant part of the ASJ neuron response. Thus, even though these signaling molecules are found in multiple cells, they are likely modulated cell autonomously. Because conventional genetic and molecular techniques are generally organismal, this underscores the importance of cell-specific manipulations such as femtosecond laser ablation in elucidating complex development and behaviors.

EXPERIMENTAL PROCEDURES

Cultivation and Strains

Following standard methods by Brenner (1974), we cultured strains (see Extended Experimental Procedures) on nematode growth medium (NGM) plates inoculated with OP50 bacteria (i.e., seeded plates), the primary food source for laboratory *C. elegans*, and

maintained animals at 15°C, unless otherwise stated. Experiments in liquid solution employed NGM buffer, which includes the same inorganic salts as NGM agar.

Surgery by Femtosecond Laser Ablation

The femtosecond laser ablation technique is a precise tool that performs submicron-resolution subcellular dissections in bulk biological tissue (Chung and Mazur, 2009). We followed established procedures for immobilization, imaging, surgery by femtosecond laser ablation, and postsurgery imaging (Chung et al., 2006). We immobilized dauers, L4s, and adults with 5 mM and L1s with 2 mM sodium azide (NaN_3). Where possible, we mixed mock (anesthetized, fluorescently imaged, but not laser irradiated) and surgery animals within batches and cultivated them together on the same plates to minimize differences, distinguishing between mock and surgery animals by postassay reimaging. All animals assayed (see below) were anesthetized and fluorescently imaged; therefore, in the text below, we employ the term “mock” only when necessary to distinguish nonsurgery animals from postsurgery animals. We targeted the ASH, ASJ, and PVQ neurons by cell-specific expression of GFP (see Extended Experimental Procedures). To target the ASK neuron, we stained animals with DiI and identified the ASK by its anterodorsal position (Herman and Hedgecock, 1990). Using a 10 kHz repetition rate, cell bodies were irradiated with 3–10 nJ pulses, whereas cilia, dendrites, and axons were irradiated with 3 nJ pulses (Figures 1 and S1). We reimaged all animals after assay and only counted animals with successful surgery and without neuronal regeneration to the nerve ring. The Extended Experimental Procedures contain more details about femtosecond laser ablation.

Assays

The Extended Experimental Procedures contain more details about the statistical tests and interpretations of results from the assays.

Osmotic Avoidance

We performed this assay as previously described (Chung et al., 2006). We performed whole-cell ablations in L1 with assay in adult stage, dendrite cuts in L4 with assay in adult stage, and axon cuts in young adult stage with assay 4 hr postsurgery to avoid axon regeneration.

Locomotion

All cultivation and assays for locomotion were performed on seeded plates at 20°C. We made every effort to measure the maximum forward crawling speed of animals during normal, spontaneous, sustained forward crawling. If animals were moved or disturbed, we waited at least 2 min to allow them to return to normal crawling. We videotaped each animal under a dissecting microscope for 3–6 min. For the experiments measuring speed during development (Figures 2B and S2A), we assayed each animal once at the given time points. For the experiment comparing different whole-cell ablations (Figure 2C), we tested each animal once at 70 hr after surgery. For the experiments comparing surgeries on different ASJ components (Figures 2D and S2B), we assayed each animal at 16, 24, and 40 hr after surgery and used the average speed. We analyzed the videos in ImageJ by measuring the total forward movement during a sustained forward run and dividing by the run duration.

Most animals with a wild-type locomotion phenotype executed runs longer than 40 s during the video; for the remaining coordinated animals, we combined together two or more of the runs to calculate the average speed over a time of more than 40 s. Severely uncoordinated mutants did not execute runs; we added together the entire forward distance moved and divided by the time of the entire movie. We did not include any backward crawling, which is significantly more efficient than forward crawling in *unc-1(e580)* mutants. The same animals were observed for all five time points, except for the 44 hr N2 data set, which occurred during the L4-adult molt and originally yielded an unusually low crawling speed. For that data set, we cultivated and processed new N2 mock animals under the same conditions as the original experiment but picked out nonquiescent animals for observation.

Dauer Entry

One day before surgery, we moved *daf-11* parent animals to the experimental temperature. We collected offspring animals within 1 hr of hatching and, unless otherwise stated, performed surgeries for dauer entry at 4 hr (25°C) or 6 hr (15°C) after hatching, when GFP labeling permitted clear imaging of neuronal fibers. After surgery (see above), we moved *daf-11* mutants to new seeded plates, where they either developed normally or into dauer. Following the established protocol of Malone et al. (1996) and Schackwitz et al. (1996), we assayed the number of animals entering dauer beginning at 42 hr after surgery to avoid counting as normal any animals that passed through dauer transiently. Dauer and older, developing animals were removed for reimaging. Younger animals were observed multiple times each day until they had developed into dauer or L4.

Dauer Exit Assay on Seeded NGM Plates

We generated wild-type and *daf-11* dauers by placing parent animals on a seeded plate at 25°C. Wild-type animals consumed the bacterial lawn and formed dauers; *daf-11* mutants entered dauer due to their dauer constitutive phenotype. We removed dauers from the plate, washed them twice in NGM buffer, performed surgery, recovered them in NGM buffer for the stated time, and returned them to seeded plates for the assay. Seeded plates were checked every hour for the first 5–6 hr and every 2 hr thereafter. Animals that had crawled up the plate sides were moved back onto the seeded agarose. We scored dauer exit by pharyngeal pumping.

Dauer Exit Assay in NGM Buffer

We generated and surgically processed dauers as above, except that wild-type dauers were starved and assayed at 20°C. We assessed dauer exit on postsurgery animals immersed in NGM buffer in 1 ml wells. Following established procedures by Bargmann and Horvitz (1991) and Cassada and Russell (1975), we kept animals for 7 hr in 0.7 ml of NGM buffer with or without 8–12 × 10^9 bacteria/ml OP50, confirmed using a cell-counting chamber. We then immersed animals in 1% SDS for 15 min and moved them to an unseeded sterile NGM plate, scoring as dauers any wild-type animals exhibiting a response to touch 1 hr after SDS treatment. Under these criteria, however, we would have scored all *daf-11* mutants as alive because they are strongly dauer constitutive. For experiments with *daf-11* mutants, we

counted as dauers any animals moving more than 2–3 cm in the hour following SDS treatment.

Supplementary Material

Refer to Web version on PubMed Central for supplementary material.

ACKNOWLEDGMENTS

Several people contributed to the work described in this paper. S.H.C. conceived the idea and carried out most of the experiments for this work; A.S. and R.C.H.R. carried out the wild-type dauer experiments in liquid solution. R.C.H.R. also performed the locomotion assays for animals processed in L4 stage. E.M. and C.V.G. supervised the research and the development of the manuscript. S.H.C. wrote the first draft of the manuscript, and all authors subsequently took part in the revision process and approved the final copy of the manuscript. We thank Cornelia Bargmann for suggesting *daf-11* dauer entry experiments and Aravinthan Samuel and Yun Zhang for supplies and technical advice. We also thank Philip Morgan, Piali Sengupta, and Joohong Ahnn for strains and guidance. Some nematode strains used in this work were provided by the Caenorhabditis Genetics Center, which is funded by the NIH National Center for Research Resources. The authors were supported in part by the Massachusetts Life Sciences Center, the National Science Foundation under contracts DMR-0213805 and PHY-0555583, and the National Institute of Neurological Disorders and Stroke, NIH under grant R21NS078580. The contents of this work are solely the responsibility of the authors and do not necessarily represent the official views of the National Library of Medicine or NIH, DHHS.

REFERENCES

Avery L, Bargmann CI, Horvitz HR. The *Caenorhabditis elegans* unc-31 gene affects multiple nervous system-controlled functions. Genetics. 1993; 134:455–464. [PubMed: 8325482]

Bargmann CI. Genetic and cellular analysis of behavior in *C. elegans*. Annu. Rev. Neurosci. 1993; 16:47–71. [PubMed: 8460900]

Bargmann CI, Horvitz HR. Control of larval development by chemosensory neurons in *Caenorhabditis elegans*. Science. 1991; 251:1243–1246. [PubMed: 2006412]

Bargmann CI, Avery L. Laser killing of cells in *Caenorhabditis elegans*. Methods Cell Biol. 1995; 48:225–250. [PubMed: 8531727]

Birnby DA, Link EM, Vowels JJ, Tian H, Colacurcio PL, Thomas JH. A transmembrane guanylyl cyclase (DAF-11) and Hsp90 (DAF-21) regulate a common set of chemosensory behaviors in *Caenorhabditis elegans*. Genetics. 2000; 155:85–104. [PubMed: 10790386]

Brenner S. The genetics of *Caenorhabditis elegans*. Genetics. 1974; 77:71–94. [PubMed: 4366476]

Campagna JA, Miller KW, Forman SA. Mechanisms of actions of inhaled anesthetics. N. Engl. J. Med. 2003; 348:2110–2124. [PubMed: 12761368]

Carroll BT, Dubyak GR, Sedensky MM, Morgan PG. Sulfated signal from ASJ sensory neurons modulates stomatin-dependent coordination in *Caenorhabditis elegans*. J. Biol. Chem. 2006; 281:35989–35996. [PubMed: 16973616]

Cassada RC, Russell RL. The dauerlarva, a post-embryonic developmental variant of the nematode *Caenorhabditis elegans*. Dev. Biol. 1975; 46:326–342. [PubMed: 1183723]

Chung SH, Mazur E. Femtosecond laser ablation of neurons in *C. elegans* for behavioral studies. Appl. Phys., A Mater. Sci. Process. 2009; 96:335–341.

Chung SH, Clark DA, Gabel CV, Mazur E, Samuel AD. The role of the AFD neuron in *C. elegans* thermotaxis analyzed using femtosecond laser ablation. BMC Neurosci. 2006; 7:30. [PubMed: 16600041]

Culotti JG, Russell RL. Osmotic avoidance defective mutants of the nematode *Caenorhabditis elegans*. Genetics. 1978; 90:243–256. [PubMed: 730048]

de Bono M, Maricq AV. Neuronal substrates of complex behaviors in *C. elegans*. Annu. Rev. Neurosci. 2005; 28:451–501. [PubMed: 16022603]

Gabel CV, Antoine F, Chuang CF, Samuel AD, Chang C. Distinct cellular and molecular mechanisms mediate initial axon development and adult-stage axon regeneration in *C. elegans*. Development. 2008; 135:1129–1136. [PubMed: 18296652]

Golden JW, Riddle DL. A pheromone-induced developmental switch in *Caenorhabditis elegans*: temperature-sensitive mutants reveal a wild-type temperature-dependent process. Proc. Natl. Acad. Sci. USA. 1984; 81:819–823. [PubMed: 6583682]

Hammarlund M, Nix P, Hauth L, Jorgensen EM, Bastiani M. Axon regeneration requires a conserved MAP kinase pathway. Science. 2009; 323:802–806. [PubMed: 19164707]

Hattori K, Inoue M, Inoue T, Arai H, Tamura HO. A novel sulfotransferase abundantly expressed in the dauer larvae of *Caenorhabditis elegans*. J. Biochem. 2006; 139:355–362. [PubMed: 16567400]

Hecht RM, Norman MA, Vu T, Jones W. A novel set of uncoordinated mutants in *Caenorhabditis elegans* uncovered by cold-sensitive mutations. Genome. 1996; 39:459–464. [PubMed: 8984009]

Herman RK, Hedgecock EM. Limitation of the size of the vulval primordium of *Caenorhabditis elegans* by lin-15 expression in surrounding hypodermis. Nature. 1990; 348:169–171. [PubMed: 2234080]

Hu, PJ. WormBook. 2007. Dauer; p. 1-19.

Li, C.; Kim, K. WormBook. 2008. Neuropeptides; p. 1-36.

Malone EA, Inoue T, Thomas JH. Genetic analysis of the roles of daf-28 and age-1 in regulating *Caenorhabditis elegans* dauer formation. Genetics. 1996; 143:1193–1205. [PubMed: 8807293]

Morgan PG, Sedensky M, Meneely PM. Multiple sites of action of volatile anesthetics in *Caenorhabditis elegans*. Proc. Natl. Acad. Sci. USA. 1990; 87:2965–2969. [PubMed: 2326259]

Ohkura K, Suzuki N, Ishihara T, Katsura I. SDF-9, a protein tyrosine phosphatase-like molecule, regulates the L3/dauer developmental decision through hormonal signaling in *C. elegans*. Development. 2003; 130:3237–3248. [PubMed: 12783794]

Pinan-Lucarre B, Gabel CV, Reina CP, Hulme SE, Shevkoplyas SS, Slone RD, Xue J, Qiao YJ, Weisberg S, Roodhouse K, et al. The core apoptotic executioner proteins CED-3 and CED-4 promote initiation of neuronal regeneration in *Caenorhabditis elegans*. PLoS Biol. 2012; 10:e1001331. [PubMed: 22629231]

Potter LR. Guanylyl cyclase structure, function and regulation. Cell. Signal. 2011; 23:1921–1926. [PubMed: 21914472]

Rajaram S, Sedensky MM, Morgan PG. Unc-1: a stomatin homologue controls sensitivity to volatile anesthetics in *Caenorhabditis elegans*. Proc. Natl. Acad. Sci. USA. 1998; 95:8761–8766. [PubMed: 9671752]

Schackwitz WS, Inoue T, Thomas JH. Chemosensory neurons function in parallel to mediate a pheromone response in *C. elegans*. Neuron. 1996; 17:719–728. [PubMed: 8893028]

Sedensky MM, Siefker JM, Morgan PG. Model organisms: new insights into ion channel and transporter function. Stomatin homologues interact in *Caenorhabditis elegans*. Am. J. Physiol. Cell Physiol. 2001; 280:C1340–C1348. [PubMed: 11287347]

Senti G, Ezcurra M, Löbner J, Schafer WR, Swoboda P. Worms with a single functional sensory cilium generate proper neuron-specific behavioral output. Genetics. 2009; 183:595–605. [PubMed: 19652182]

Strott CA. Sulfonation and molecular action. Endocr. Rev. 2002; 23:703–732. [PubMed: 12372849]

Thomas JH. Chemosensory regulation of development in *C. elegans*. Bioessays. 1993; 15:791–797. [PubMed: 8141797]

Thomas JH, Birnby DA, Vowels JJ. Evidence for parallel processing of sensory information controlling dauer formation in *Caenorhabditis elegans*. Genetics. 1993; 134:1105–1117. [PubMed: 8375650]

Tissenbaum HA, Hawdon J, Perregaux M, Hotez P, Guarente L, Ruvkun G. A common muscarinic pathway for diapause recovery in the distantly related nematode species *Caenorhabditis elegans* and Ancylostoma caninum. Proc. Natl. Acad. Sci. USA. 2000; 97:460–465. [PubMed: 10618440]

Vowels JJ, Thomas JH. Genetic analysis of chemosensory control of dauer formation in *Caenorhabditis elegans*. Genetics. 1992; 130:105–123. [PubMed: 1732156]

Vowels JJ, Thomas JH. Multiple chemosensory defects in daf-11 and daf-21 mutants of *Caenorhabditis elegans*. Genetics. 1994; 138:303–316. [PubMed: 7828815]

Wang J, Kim SK. Global analysis of dauer gene expression in *Caenorhabditis elegans*. Development. 2003; 130:1621–1634. [PubMed: 12620986]

White JG, Southgate E, Thomson JN, Brenner S. The structure of the nervous system of the nematode *Caenorhabditis elegans*. Philos. Trans. R. Soc. Lond. B Biol. Sci. 1986; 314:1–340. [PubMed: 22462104]

Wollam J, Antebi A. Sterol regulation of metabolism, homeostasis, and development. Annu. Rev. Biochem. 2011; 80:885–916. [PubMed: 21495846]

Zallen JA, Kirch SA, Bargmann CI. Genes required for axon pathfinding and extension in the *C. elegans* nerve ring. Development. 1999; 126:3679–3692. [PubMed: 10409513]

Zhang M, Chung SH, Fang-Yen C, Craig C, Kerr RA, Suzuki H, Samuel AD, Mazur E, Schafer WR. A self-regulating feed-forward circuit controlling *C. elegans* egg-laying behavior. Curr. Biol. 2008; 18:1445–1455. [PubMed: 18818084]

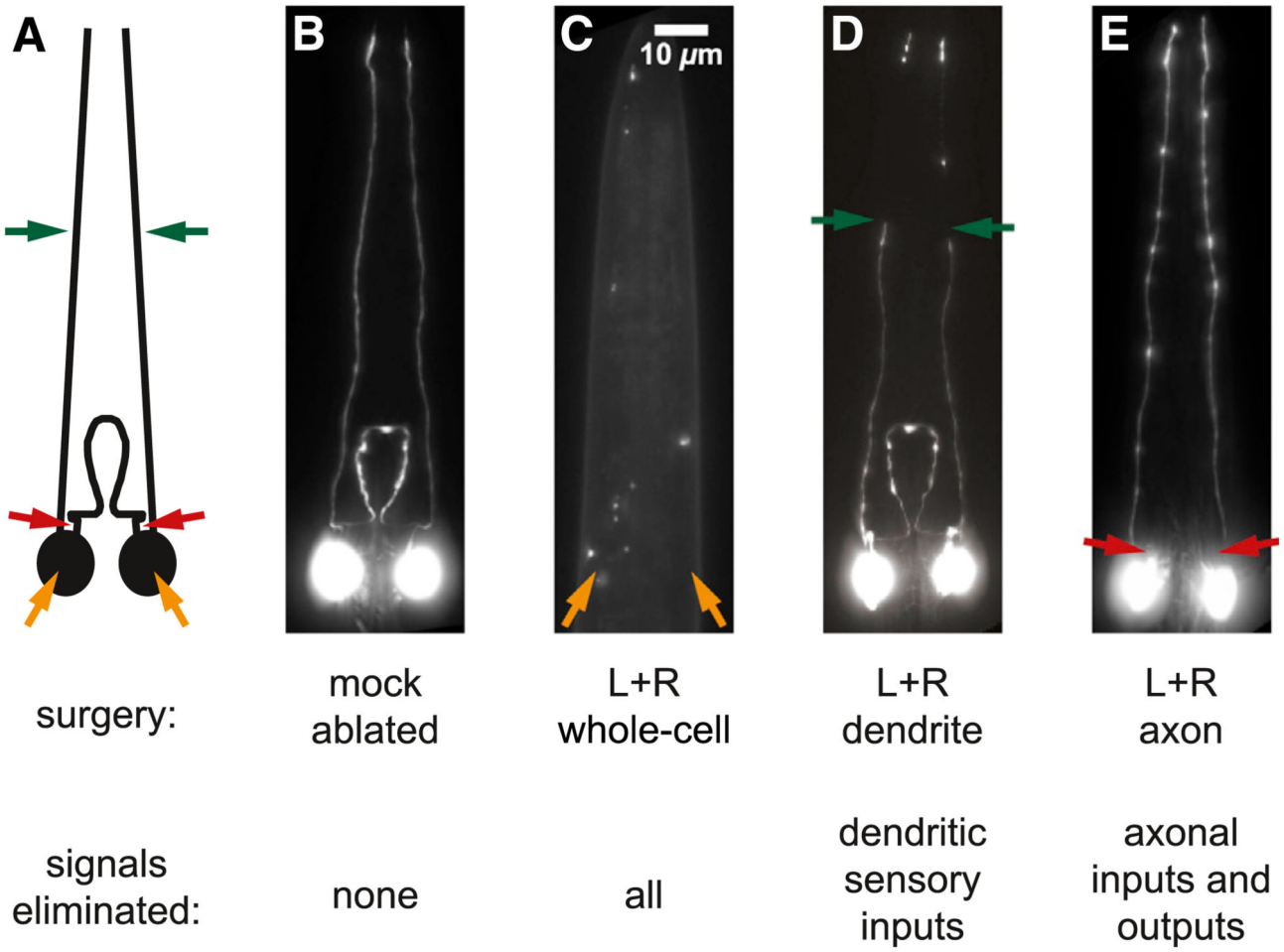

Figure 1. Imaging and Behavioral Assay Confirm Systematic Femtosecond Laser Ablation of Amphid Neuron Subcellular Components

(A–E) GFP fluorescence images 2 days after L+R ASJ surgeries in L1. Colored markers indicate location of surgeries.

(A) Line drawing of ASJ neurons.

(B) Mock surgery.

(C) Whole-cell ablation.

(D) Dendrite cut.

(E) Axon cut.

See also Figure S1.

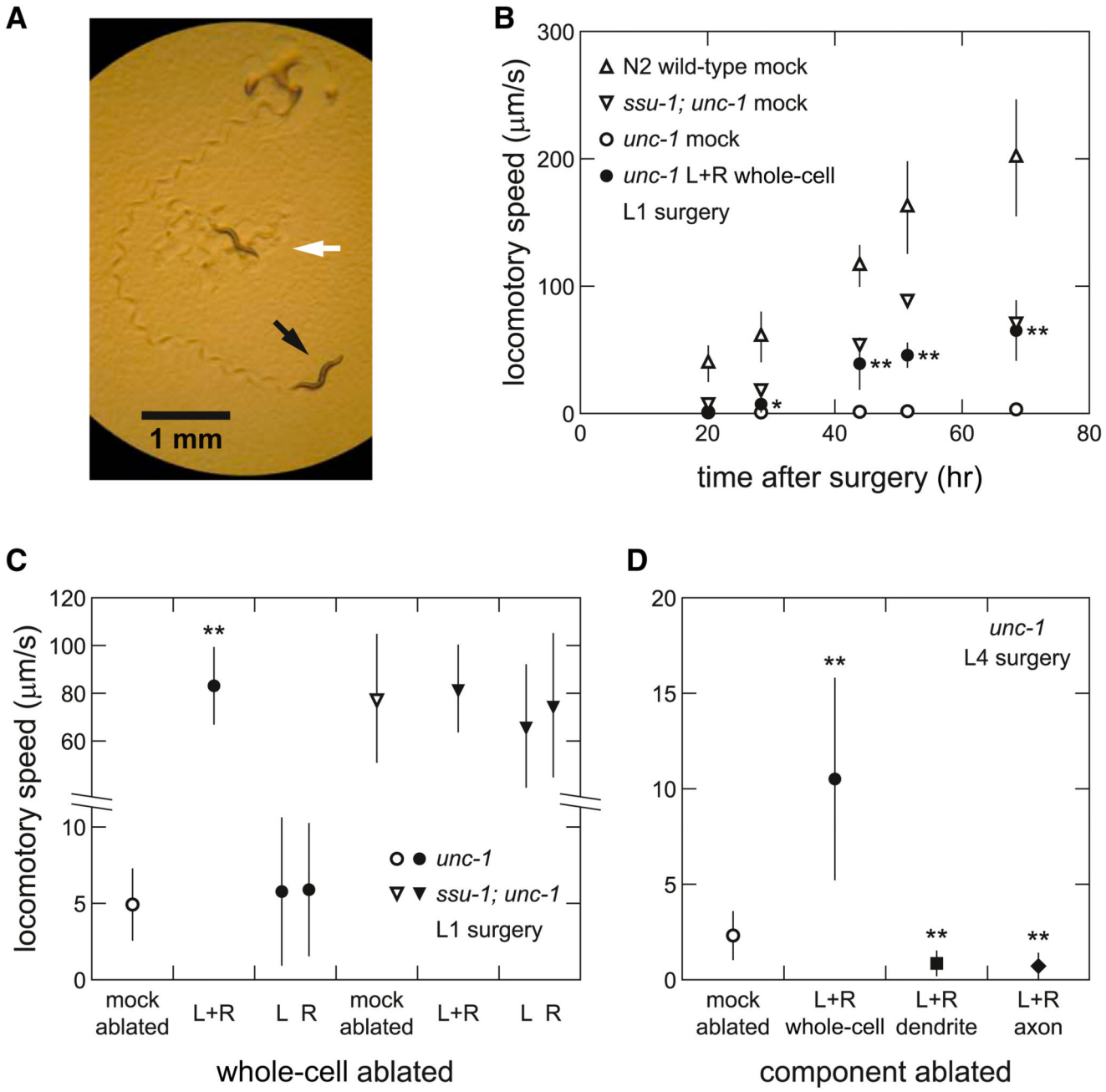

Figure 2. ASJ Cell Body Mediates the *unc-1* Locomotion Phenotype

(A) Crawling tracks on seeded plates of *unc-1* mutants 2 days after ablation or mock ablation of L+R cell body within 7 hr of hatching. Postsurgery animal (black arrow) introduced to plate less than 1 min prior to photographing crawls around mock animal (white arrow) introduced to plate over 1 hr prior to photographing.

(B) Postsurgery crawling speeds of various strains. *ssu-1; unc-1* error bars, which are similar in magnitude to and overlap with postsurgery error bars, are not shown for simplicity. (Mock) surgery performed within 2 hr of hatching ($7 \leq n \leq 19$).

(C) Crawling speed of *unc-1* and *ssu-1; unc-1* mutants 3 days after whole-cell ablation in L1 stage ($19 \leq n \leq 24$, except for *ssu-1; unc-1* L or R ablations, where $n = 7$).
(D) Crawling speed of *unc-1* mutants 2 days after surgery in late L4 stage ($13 \leq n \leq 37$).
Data are represented as mean ± SD.
See also Figure S2.

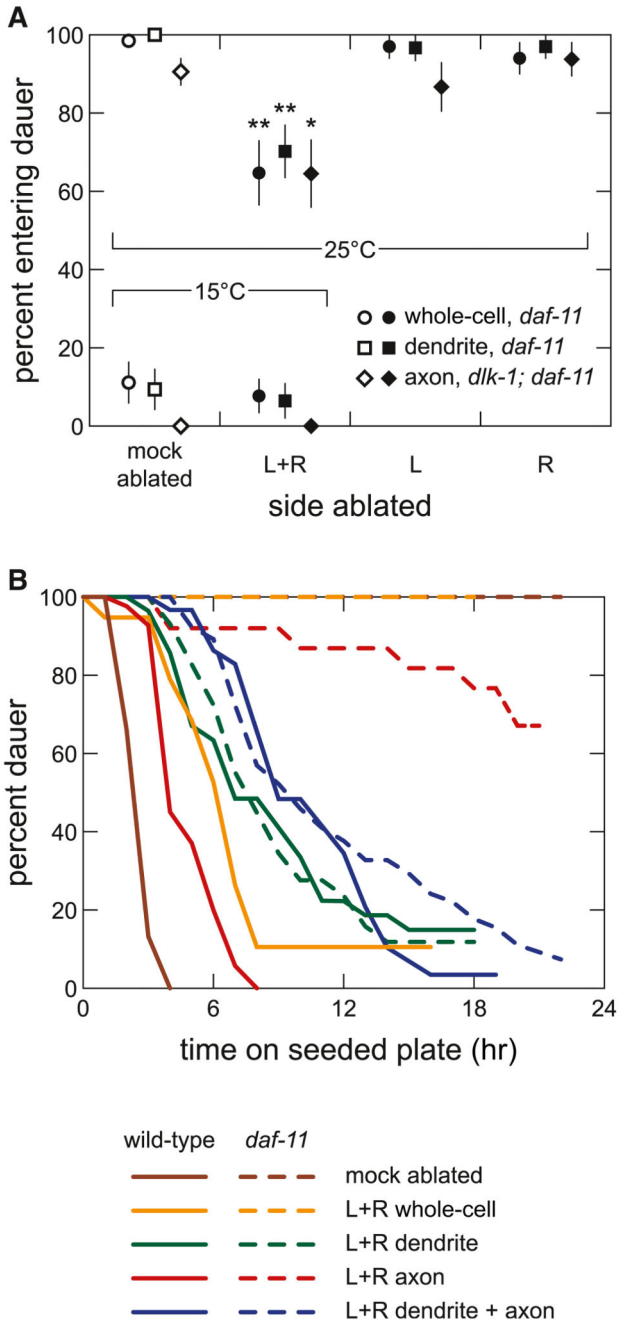

Figure 3. Dauer Entry and Exit Behaviors after ASJ Surgeries

(A) ASJ cell body, dendrite, and axon mediate *daf-11* dauer entry behavior. Top view shows dauer entry of *daf-11* mutants at 25°C (whole cell and dendrite) and *daf-11; dlk-1* mutants at 24.5°C (axon) after various surgeries at 4 hr posthatch. L+R surgeries yield significant decrease of dauer entry, compared with corresponding mock animals, whereas single-sided surgeries do not. Bottom view shows dauer entry of *daf-11* mutants (whole cell and dendrite) and *daf-11; dlk-1* mutants (axon) at 15°C after surgery at 6 hr posthatch. Filled markers are surgeries, and open markers are corresponding mock animals ($30 \leq n \leq 74$).

(B) ASJ cell body, dendrite, and axon contribute to dauer exit behavior. Dauer exit of wild-type and *daf-11* animals on seeded plates after L+R surgery. Curves show the percentage of animals remaining in dauer after elapsed time on plate at 25°C ($19 \leq n \leq 68$). All surgery data sets, except *daf-11* L+R whole-cell ablation, differ from their corresponding mock data sets at $p < 10^{-4}$. See also Figure S3.

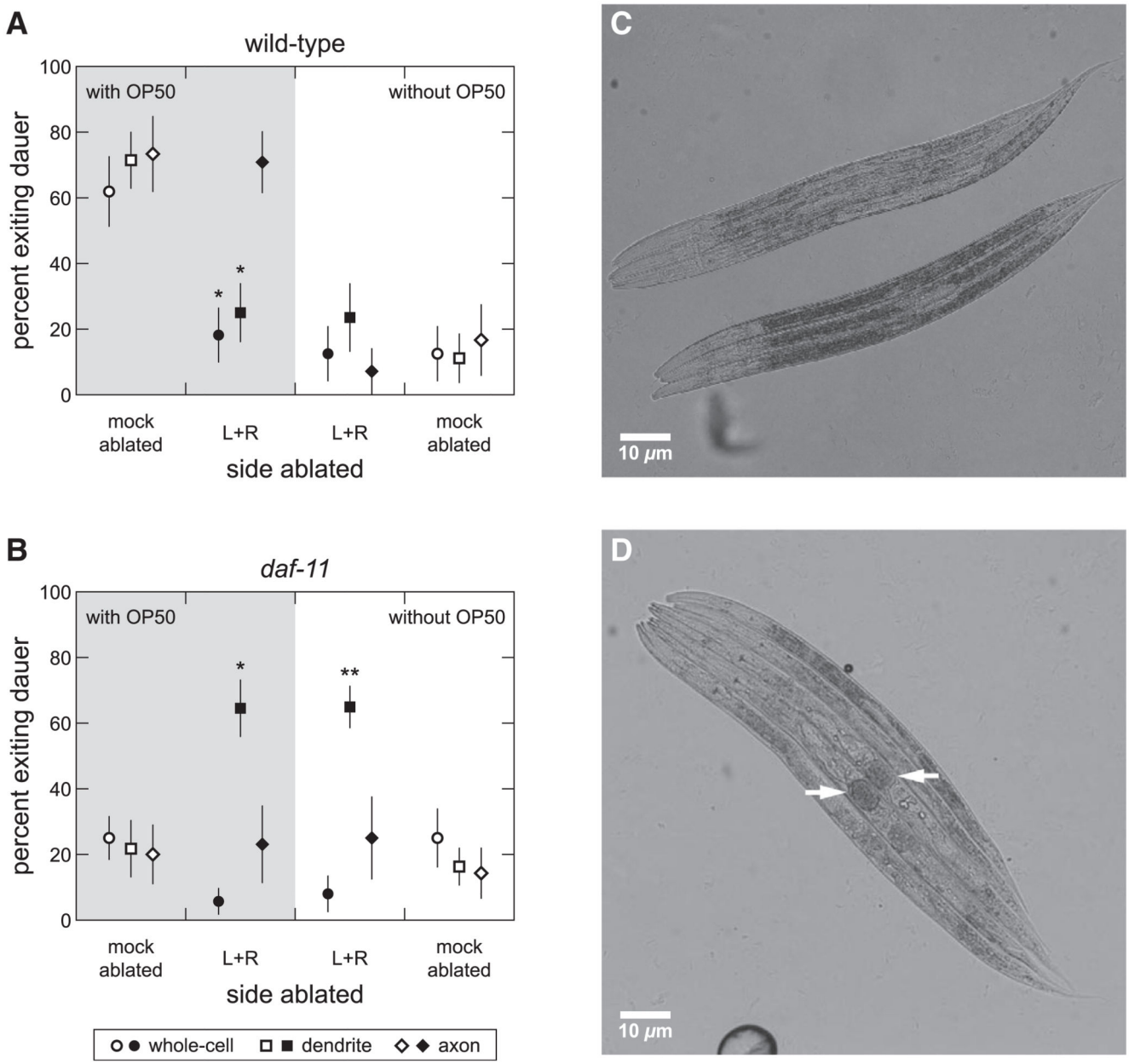

Figure 4. ASJ Involvement in Dauer Exit without Food

(A and B) Percentage of wild-type (A) and *daf-11* (B) animals exiting dauer in NGM buffer with (shaded) and without (clear) OP50 after indicated surgeries of L+R ASJ components. Circles are whole-cell ablation, squares are dendrite-cut, and diamonds are axon-cut data. Filled markers are surgeries, and open markers are corresponding mock animals ($12 \leq n \leq 57$). Data are represented as mean ± SD.

(C) *daf-11* mutants kept in NGM buffer without OP50 for 1 day after surgery. L+R dendrite-cut animals (top three) are noticeably paler than mock animals (bottom three), indicating initiation of dauer exit.

(D) L+R dendrite-cut *daf-11* mutants kept in NGM buffer without OP50 for 3 days after surgery. Lower four animals have exited dauer, and lower three animals have continued development; two animals are producing eggs (arrows).

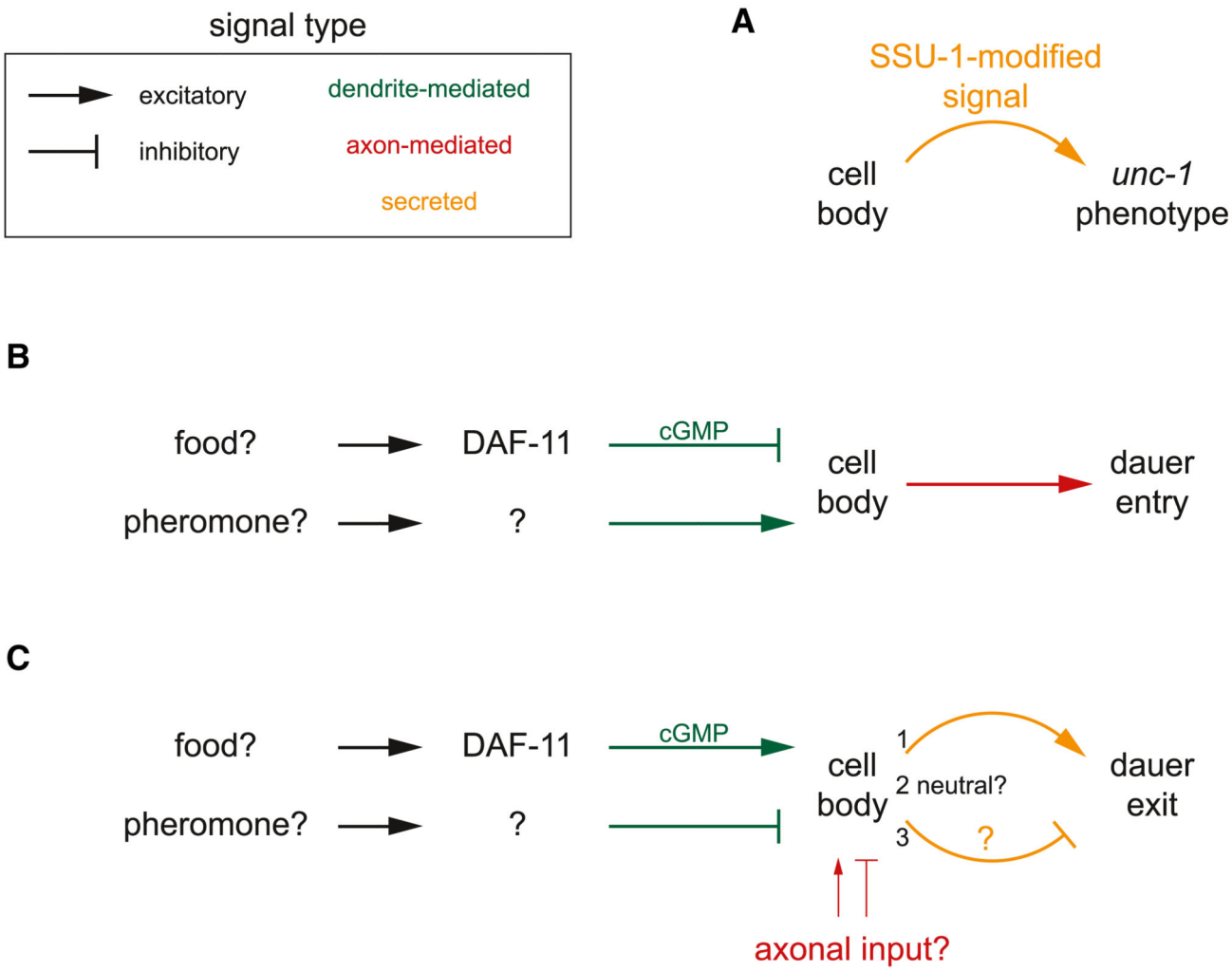

Figure 5. Working Models of ASJ Signaling in Locomotion, Dauer Entry, and Dauer Exit

Arrows indicate excitatory signals, and bars indicate inhibitory signals. Dendrite-mediated signals are in green, and axon-mediated signals are in red. Curved lines (orange) indicate a signal secreted by the cell body. Sizes of the arrows and bars indicate the relative effect of signal on dauer behavior.

(A) ASJ signaling for locomotion. The cell body mediates the *unc-1* phenotype by secreting an SSU-1-modified signal.

(B and C) ASJ signaling for dauer entry and exit. The dendrite transmits excitatory and inhibitory signals to the cell body that switch polarity between entry and exit and primarily drive the cell body's role in dauer behavior. Food and pheromone environmental cues may be transduced in the ASJ cilia by DAF-11 and putative pheromone receptor(s), respectively. (B) The cell body sends out an axonally mediated signal promoting dauer entry. (C) The cell body can be neutral toward or can secrete signals to promote or repress dauer exit. Because the ASJ cell body both promotes and represses dauer exit, the signs of the dendritic signals indicate their effect on dauer exit, not the cell body.

Table 1
Sign of the ASJ Dendritic Signal for Dauer Decisions

Row	Background	Behavior	Pheromone	Food	Dendritic Signal	Citation
1	Wild-type	Entry	No	Yes	−?	Vowels and Thomas, 1992
2	*daf-11*	Entry	No	Yes	+?	Vowels and Thomas, 1992
3	Wild-type	Entry	Yes	Yes	+?	Vowels and Thomas, 1994
4	*daf-11*	Entry	No	Yes	+	This work
5	Wild-type	Exit	No	Yes	+	This work
6	*daf-11*	Exit	No	Yes	−	This work
7	Wild-type	Exit	No	No	−	This work
8	*daf-11*	Exit	No	No	−	This work

Rows 1–3 summarize published results. Rows 4–8 summarize our results from various assays after L+R dendrite surgeries. For each experiment, we list the genetic background, the behavior (dauer entry or exit), the environmental conditions (applied pheromone and/or OP50 bacteria food), and whether the defined dendritic signal promotes (+) or inhibits (−) the behavior.